

UNCLASSIFIED

Defense Technical Information Center
Compilation Part Notice

ADP010638

TITLE: Damage Tolerance to Low Velocity Impact of
Laminated Composites

DISTRIBUTION: Approved for public release, distribution unlimited

This paper is part of the following report:

TITLE: Application of Damage Tolerance Principles
for Improved Airworthiness of Rotorcraft
[l'Application des principes de la tolerance a
l'endommagement pour une meilleure aptitude au
vol des aeronefs a voilure tournante]

To order the complete compilation report, use: ADA389234

The component part is provided here to allow users access to individually authored sections of proceedings, annals, symposia, ect. However, the component should be considered within the context of the overall compilation report and not as a stand-alone technical report.

The following component part numbers comprise the compilation report:

ADP010634 thru ADP010648

UNCLASSIFIED

DAMAGE TOLERANCE TO LOW VELOCITY IMPACT OF LAMINATED COMPOSITES

G A O Davies, D Hitchings and X Zhang

Department of Aeronautics, Imperial College, South Kensington, London SW7 2BY, UK

Abstract

A strategy is developed for predicting easily the threshold energy for delamination caused by impact, whatever the nature of the laminated structure. The actual delamination and fibre damage is also predicted and the consequent compression-after-impact strengths. The latter strategies may be approximate but current research is pointing the way to more accurate solutions based on finding energy-release-rates around the delamination front.

1. Introduction

This specialist meeting is concerned with damage tolerance in helicopter structures. As the helicopter is an ideal fatigue machine and as most helicopter structures are still metallic (excluding rotor blades) it is natural that the emphasis should be on improving tolerance to cyclic loading and in using modern damage-tolerant methods to assess the time in which an inspectable crack will grow to an unstable situation which puts the structure at risk.

This paper is however aimed at laminated composite structures which have their own brand of damage susceptibility and which is serious without the threat of cyclic loading (indeed carbon-epoxy composites have a rather good fatigue performance compared with metals) and that is the threat of impact damage. It will become increasingly important as more helicopter fuselages and empanages are built out of carbon-epoxy materials: the Bell 427 for example has 70% composite airframe structure.

The effect of impact damage, particularly on the compressive strength of aircraft structures, has been known for more than 15 years. The traditional way of coping with impact damage has been to limit design allowable strains in compression to 0.3% or thereabouts, whereas the material can probably take 0.8% at least if dry at room temperature. Countless coupon tests have shown alarming reductions in the compression-after-impact (CAI) strength. Figure 1 shows the reduction of 70% for a thermoset resin, and less so for a thermoplastic. The second figure shows that the reduction in strength appears to be insensitive to the impact site (more of this later). Such tests on coupons are useful for comparing different materials for example, but are unsuitable for real structures where the nature of the structure can radically alter the amount of damage, depending as it does on the history of the impact force and structural strains during the impact event. These will depend on the dynamic response which will in turn depend on the structural mass, stiffness, geometry, sub-structure, internal stress field etc. A flexible structure may not be as badly damaged as a locally stiff one for example. How then does one assess the amount of impact damage in a real structure without conducting a large set of very expensive impact tests, and in particular how to do this during the design phase when damage tolerance may be a key issue?

2. The Nature of Low-Velocity Impact Damage

This paper concentrates on low velocity impact which may cause significant damage by delamination in the middle region of a thin plate or it may cause tensile matrix and fibre failure on the back face, both of which are invisible to the outside observer. Barely visible impact damage (BVID) is a hidden menace. The aim is to have a – hopefully simple – analytical tool for predicting impact damage and the consequent Compression-After-Impact (CAI) strength.

Firstly it is necessary to define “low velocity”. If the incident velocity is high enough (say ballistic or rotor blade damage) then high energy stress waves are set up through the thickness of the structure, sufficient energy may mean complete penetration, and the structural response will be very local and uninfluenced by the nature of the surrounding structure. Crudely it can be shown that these stress waves give rise to a strain of order V/C , where V is the impactor velocity and C is the speed of sound through the plate thickness – governed primarily by the density and modulus of the resin matrix. Local failure will occur if these strains are of order (say) 1%. Now for epoxy resins C is of order 2000m/sec which gives the threshold for V as 20m/sec. This is not commonly thought of as low, but experiments [Ref. 1] have shown a transition from low velocity behaviour, when the thin plate has time to respond away from the impact site, when the velocity increases from roughly 20 to 60 m/sec. Accidents like tools dropped from heights up to 4m correspond to impact velocities up to 9 m/sec. It is these that form the scope of this paper.

Figure 2 shows three zones of damage developing as the plate deforms under impact. The bending strains cause (1) tensile failure on the back face in which matrix cracks occur first (and then precipitate local delamination where the cracks meet an interface) and (2) delamination in the interior where the shear strains are a maximum and finally (3) compressive strains on the impacted surface. There may also be point (HERTZIAN) damage which is very local and does not debilitate the structure much, although up to 10% of the energy may be absorbed in this mode if the impact force is high. As far as the CAI strength is concerned, the internal delamination is the main threat, since the separated laminae may buckle locally and this local blister can then propagate. The distribution of these shear-driven delaminations can be complex, consisting of a series of overlapping oblongs or “peanuts” aligned in the direction of the fibres on the lower surface. Figure 3 shows an X-ray which reveals these multi-level delaminations. However, for this particular laminate with a quasi-isotropic stacking sequence $(+45, -45, 0, 90)_{4S}$, the envelope of the delamination is circular as revealed in the C-scan shown. Also can be seen the elongated delamination in the $+45^\circ$ direction, caused by tensile matrix cracking on the back face lamina. If we use the area enclosed by the envelope as a measure of the damage, we can construct a map of impact damage with incident energy. A very large number of tests were conducted [Ref. 2] on a variety of plates having quasi-isotropic lay-ups, thicknesses 1, 2, and 4 mm, dimensions ranging from 75 x 125mm (the so-called Boeing test specimen) to 200 x 200mm, with various boundary conditions, and including a few stiffened panels impacted between stiffeners. A map of damage against the incident energy is shown in Figure 4(a) to be chaotic, and illustrates the futility of using coupons to explain everything. It was thought at one stage that this sort of scatter should be attributed to variability in the composite structures’ properties.

A very simple strategy can now be used to remove the effect of different dynamic responses of the many sizes of structure. We assume that the internal delamination is driven by shear stresses which are proportional to the impact force, and that, there is no coupling between the force history and the history of the bending strains (this turns out later not to be true). The force history was monitored during these impact tests and if we then plot damage against maximum force, the picture changes dramatically as shown in Figure 4(b). There are clearly three separate maps depending on the thickness only, and equally important the damage area for any particular plate thickness can occur anywhere in the zone band. It should therefore be possible to conduct just one set of coupon tests and use this map to predict the damage in any size of structure provided that the impact site is not near or over a local substructure. Thus the effect of dynamic response has been removed.

3. Prediction of Damage Threshold

Having shown that the damage depends primarily on the maximum impact force it is now tempting to try and predict what is clearly a threshold force, below which no damage occurs at all. One route is to model the laminated plate using a very fine finite element mesh and then solve the equations of motion to reconstruct the damage evolution during the impact event. If no approximations are to be made this means using finite elements as one brick element per lamina, so that if (say) the plate is 6mm thick (48 ply) and the damage zone is 20mm x 20mm (which is not large) we then need $48 \times (20 \div 1/8)^2 = 1.3M$ elements. Although not difficult to set up this model, this is a very expensive simulation, and more importantly it will be extremely difficult to understand the answers and the underlying physics, possibly more difficult than interpreting experimental results. Nevertheless at Fort Worth Bell Textron Helicopters are trying this out. They are also using strength criteria which we now show to be flawed.

Suppose we attempt to use the interlaminar shear strength as a failure criteria, then the mean shear stress is a simple function of force and radius (stress = $P/2\pi r t$) and hence the area πr^2 , varies continuously with P , quite unlike Figure 4(b). We therefore resorted to fracture mechanics which are capable of explaining sudden unstable propagation, and we are able to show that there is indeed a critical threshold force P_{crit} at which delamination will occur, and that this is independent of radius of the delamination circle [Ref. 3]

$$P_{crit}^2 = \frac{8\pi^2 Et^3 G_{IIC}}{9(1-\nu^2)} \quad (1)$$

Notice that this force is a function of the plate stiffness (Et^3) and the mode II fracture toughness G_{IIC} , explaining why thermoplastics are less susceptible to damage since the fracture toughness may be two or three times that of a thermoset. Equation (1) is based on the highly simplifying assumption that the damage and the structural strains are axis-symmetrical which is approximately true for a quasi-isotropic lay-up, nevertheless Figure 5 shows that this equation is a reasonably accurate predictor. Thus if we wish to avoid delamination completely it is only necessary to find the maximum impact force and then use equation (1).

If we need only the force, and not a detailed history of the interior strain field, it is tempting to model the system as one degree of freedom – an impactor mass and a structural spring. This should be a reasonable model if the mass is heavier than the responding structure (which is likely) so that the

structures' inertia forces can be ignored. The structure should then respond in a fundamental mode and simple harmonic motion ensures that the maximum force is readily evaluated. The computing effort would be negligible since a simple static solution would give the required equivalent spring stiffness. This approach has naturally been tried by many investigators [Ref. 4]. Unfortunately there are two reasons why this may not work. Firstly the response of a real structure with discontinuities in stiffness may not be a single fundamental mode, and a mixture of harmonics may respond with no guarantee that the force history is sinusoidal with a clear maximum. Figure 6 illustrates just this point. A composite panel, 250mm x 250mm was supported as shown along four supports typical of the wing surface of a military multi-spar structure. The response in 6(a), using an impactor mass six times the panel mass, is far from sinusoidal (the peak and period are also wrongly estimated by the dynamic finite element solution due to damping at the four supports not being modelled correctly) contrast this behaviour with the same laminated plate stacking sequence but impacted in the much smaller standard Boeing rig, whose mass is now only 1/30 that of the impactor. A sinusoidal response would be an accurate approximation.

The other error source lies in ignoring the coupling between the bending strains and the shear-driven force response. If the plate is flexible enough, and if the incident energy is sufficiently high, then the bending strains may exceed the fibre allowable strengths and failure will then decrease the flexural rigidity locally and hence attenuate the force. To model this we presently need to use a finite element code, but there is no need to deploy an expensive model. In FE77 [Ref. 5] simple composite shell elements are used to assume the strain distribution through the shell thicknesses, as usual, linear, but each lamina at every level is monitored during the impact event, and if a conventional strain criteria [Ref. 6] is exceeded this element layer is deleted. The result is a quite gradual decrease in stiffness which has been shown to give force histories agreeing very well with many tests, sizes, and materials. Figure 7 shows the results of two such drop tests on the Boeing test specimens with (a) modest and (b) large incident energies. The C-scans show a conventional shear-driven circular enveloped for (a) but for (b) there is much delamination in the 45° direction under the laminate near the tensile back surface, which is a consequence of the massive matrix cracking in this region. The deflection in both cases exceed the plate thickness of 1mm and hence the code needed non-linear stiffness updates, but it also had the laminate-strength failure routine here referred to as "degraded" capability. The need for this is clear in Figure 7 (b) where the elastic undamaged prediction of 2400N is twice that of the true value of 1200N. It does look therefore that some FE modelling is unavoidable even if we wish only to find the force history and the threshold for delamination.

4. Prediction of Damage Extent

A thin-walled composite structure will still have residual compressive strength even when damaged, and there is therefore an incentive to predict the extent of this delamination even though Figure 5 has indicated the amount may be indeterminate as unstable fracture occurs. At the moment there does seem to be no alternative to using a non-linear dynamic finite element code to predict delamination, and also flexural degradation. This is nowadays accepted in crashworthiness studies on metal aircraft and automobiles, and DYNA 3-D (to name one) has become common usage in car and aero-engine impact studies. The problem in laminated

composites has been noted as the complex nature of the impact-induced delaminations. It will undoubtedly become routine as computing power becomes remorselessly cheaper and more accessible, and the commercial codes become more user-friendly in displaying damage and using it as an input to a residual CAI strength predictor. In the meantime we have assessed the accuracy of using a simpler description of damage. Using the success of the single equivalent circular delamination which led to equation (1) we assumed this form *ab initio*. Thus a delamination level was assumed and just two layers of shell elements arranged each side of it, with fictitious links joining the element node points, and which could be broken as the equivalent forces reach a value derived from the interlaminar shear strength or the peeling strength. This should predict the initiation of delamination but we need a fracture (energy release rate) criteria to propagate. The results were encouraging as Figure 8 indicates.

A more ambitious study was the damage threshold for impact over a stiffener in a top-hat stiffened compression panel. This is much more complex and not amenable to the simple analysis used for plate impact. Here the structure is locally very much stiffer than a single plate thickness and hence a much higher impact force is generated for a given energy. However a structure is better able to resist such a force since it will locally behave like a stiff beam many times stiffer than the thin plate, hence we may expect a higher threshold energy, in this case 9J. However, as Figure 9 shows the shear stress rises to a peak and is then constant along the stiffener all the way to the nearest support, there being virtually no diffusion to the surrounding panel. This is potentially very dangerous as complete separation of a stiffener can reduce the buckling load of the stiffened panel by 75%. However as is indicated in 9(a) we need to unpick nodes and establish the energy release rate to see if the peak shear of 83MPa will propagate along the stiffener. This code development is underway.

5. Compression After Impact Evaluation

Knowing the damage extent, we can feed this into a FE code which is capable of predicting the propagation of delamination when the structure is loaded in compression. The initial buckling of the delaminated zone is straightforward (Figure 10) but this local "blister" will move no further until the applied load is increased and the blister forces and moments around its periphery increase with load until there is a point at which the potential energy release rate G at some point exceeds the fracture toughness, G_c , and propagation occurs. G is predominantly mode I (peeling) but the critical value may be a combined form of mode I and mode II release rates. In the case shown the energy release rate is a maximum at the two extremities of the transverse axis of the blister so it will propagate at right angles to the applied load direction. Two methods are available for evaluating G . One is the virtual crack extension or closure in which the perimeter edge forces do work over a test perturbation of the delamination. The other is the use of hypothetical interface elements which may be thought of as representing an adhesive but whose force/displacement law is stipulated to contain G as the work done when the crack moves [Ref. 7]. Unfortunately both of these methods require a very fine mesh to evaluate G accurately and they need to be updated as the front propagates. This is a non-trivial task, and the strategy is the subject of a current research programme ADCOMP supported by the European Union. There is however an alternative, very much cheaper way, [Ref. 8] which make the unlikely assertion that a delamination zone can be approximated by a clean circular hole of the same area. This latter problem can be solved using

a fracture mechanics approach but deploying the kink-band failure mode known to be the dominant mode of failure in compression. Figure 11 shows the success of this approximation. Thus there is no easy route through

impact → damage → CAI strength,

but the physics is clearly being modelled correctly, i.e. mode II is the dominant creator of delamination damage whilst mode I is the dominant CAI failure mechanism. This should be borne in mind when the damage tolerance is to be improved by stitching, Z-pins, or a tougher resin.

6. Cyclic Loading

The propagation of delamination under cyclic loading can be simulated using the well known Paris law if we can evaluate G , and therefore the stress intensity factor K . Figure 12 shows how this is done [Ref. 9] but it needs to be said that the same fine mesh restriction is necessary once more. Work to be done is to incorporate a mixed mode I plus II law and a mixed damaged zone due to shear and peeling stresses.

7. Conclusions

The traditional industrial way of finding damage tolerance has been to establish CAI strength against impact energy using tests of coupons or components. It is clear that this can be simulated with one extra stage.

$$\frac{1}{2}mV^2 \rightarrow \text{damage extent} \rightarrow \text{CAI strength}$$

The effect of size and all the other scale effects can be eliminated by converting energy to maximum impact force. This is all that needs to be done if the threshold delamination is sufficient. If the energy is greater than this threshold then current research points the way to evaluating the damage extent and the consequent CAI strength.

8. Acknowledgements

Most of this work has been supported by the Defence Research Agency in the UK, British Aerospace (Military and Aerostructures) and by the European Union, and their help is very gratefully acknowledged.

9. References

- [1] Godwin W. and Davies G.A.O. "Impact behaviour of thermoplastic composites". CADCOMP 88, Southampton (April 1988).
- [2] Davies G.A.O. and Zhang X. "Impact damage prediction in carbon composite structures". Int. Jnl. Impact Engng., **16**, 1, pp149-170 (1995).
- [3] Davies G.A.O. and Robinson P. "Predicting failure by debonding/delamination". AGARD Conference Proceedings 530.
- [4] Abrate S. *Impact on composite structures*. Pub. C.U.P. ISBN 0521 473896 (1998).
- [5] Hitchings D. "FE77 general purpose modular finite element system for static and dynamic, linear and non-linear analysis". Dept. of Aeronautics, Imperial College (1993).
- [6] Chang F-K. and Chang K-Y. "A progressive damage model for laminated composites containing stress concentrations". Jnl. Composite Materials, **21**, pp834-855 (1987).

- [7] Mi Y., Crisfield M.A. and Davies G.A.O. "*Failure modelling in composite structures*". 5th ACME Conference, Ed. Crisfield, Imperial College, (April 1997).
- [8] Soutis C., Curtis P. and Fleck A. "*Compression failure of notched carbon fibre composites*". Proc. Roy. Soc. (A), **440** (1993).
- [9] König M and Krüger R. "*Delamination growth under cyclic loading*". ECCM-8, Naples, June (1998).

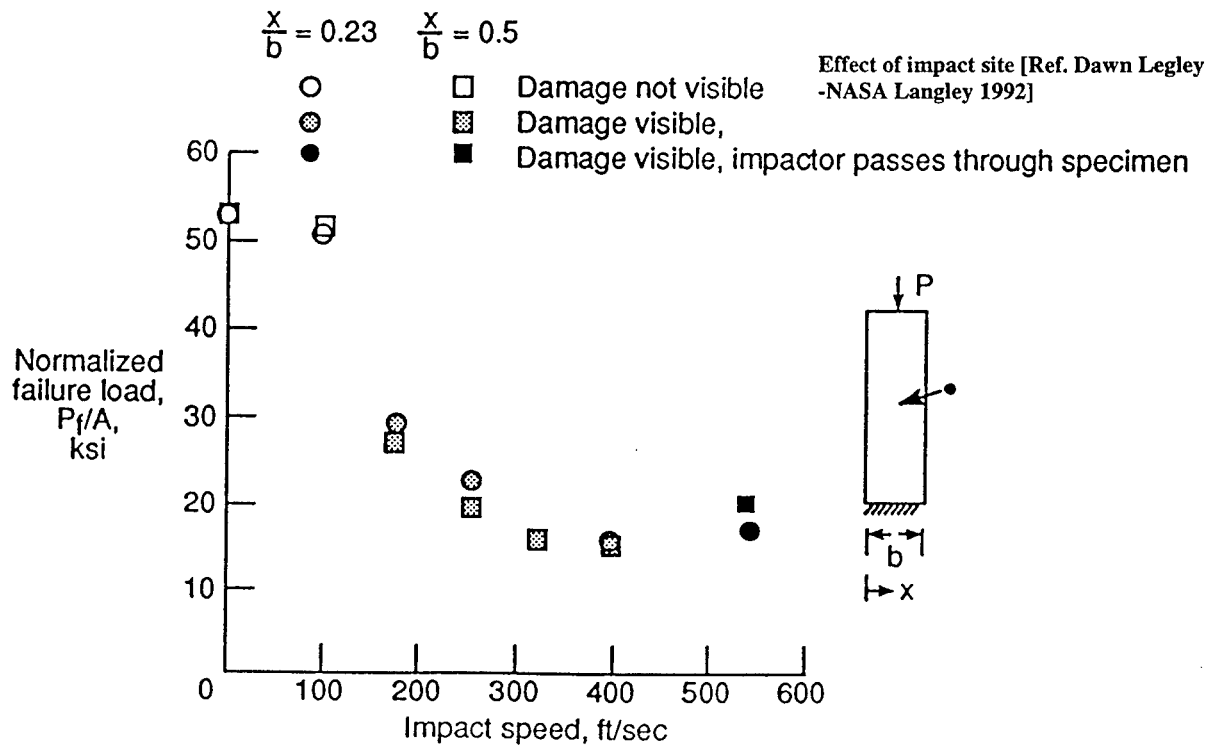
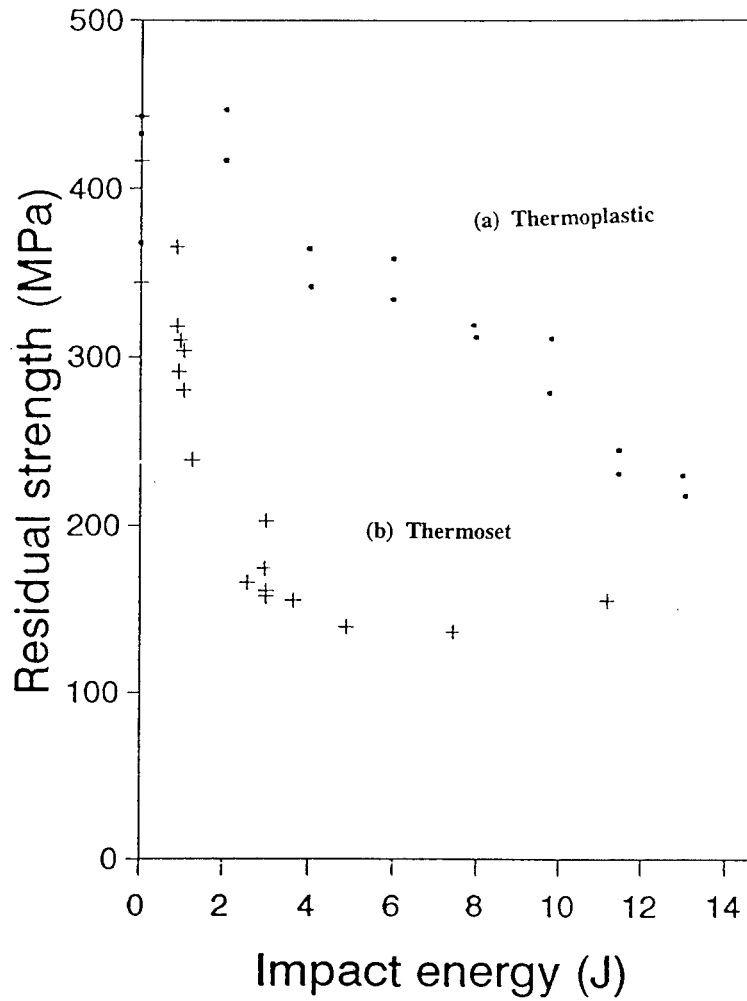


Figure 1 Compression strength after impact

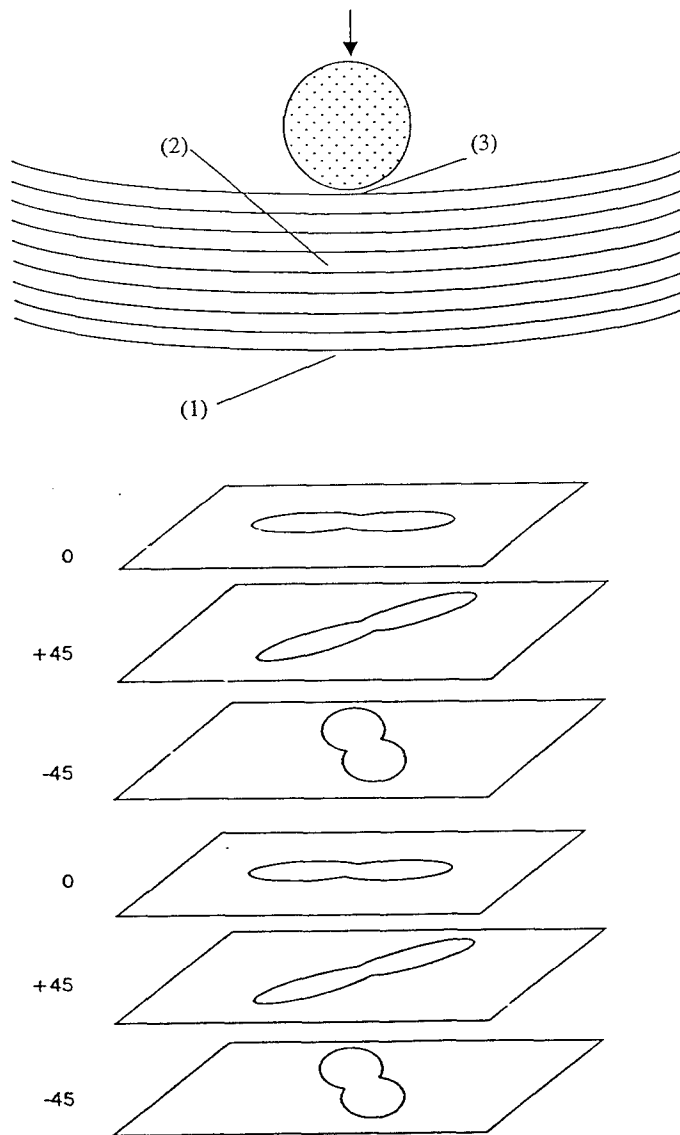


Figure 2 Low velocity impact damage zones

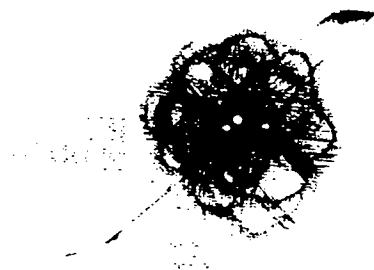
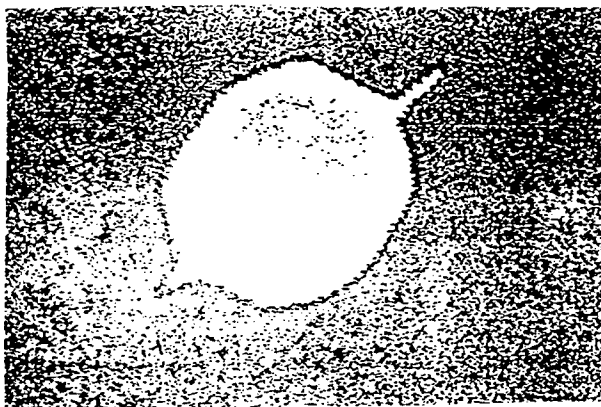


Figure 3 Internal delamination in the form of overlapping peanut shapes

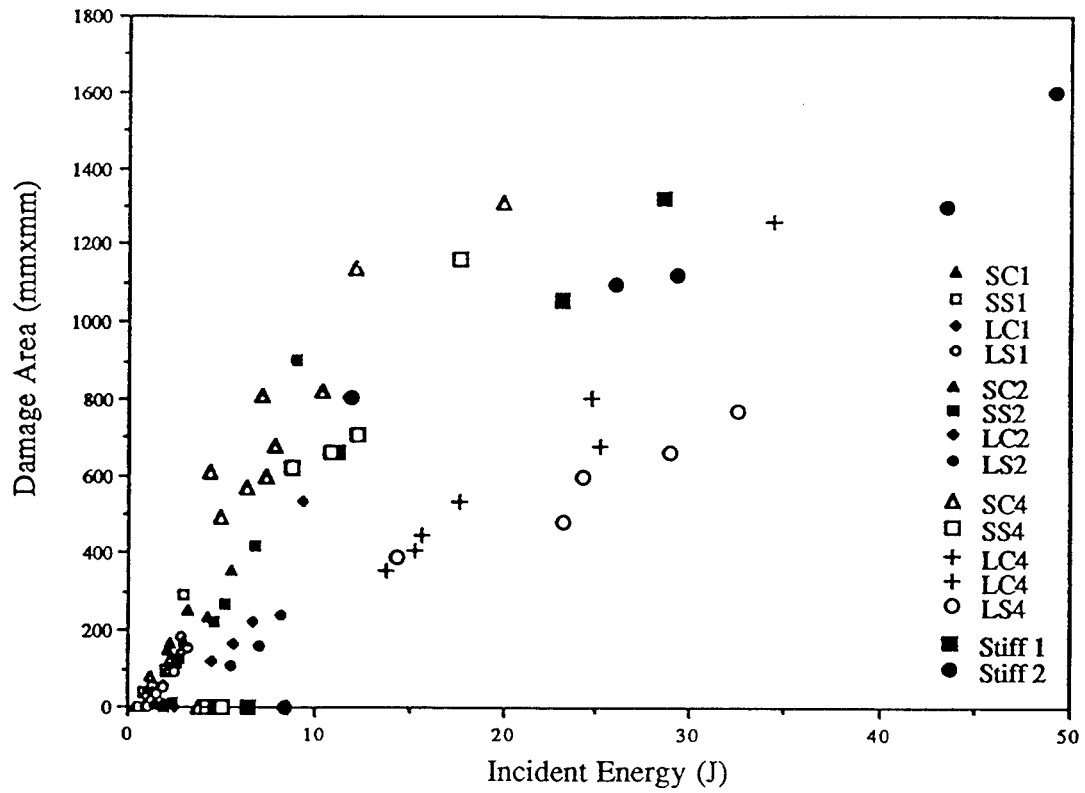


Figure 4(a) Map of damage against energy

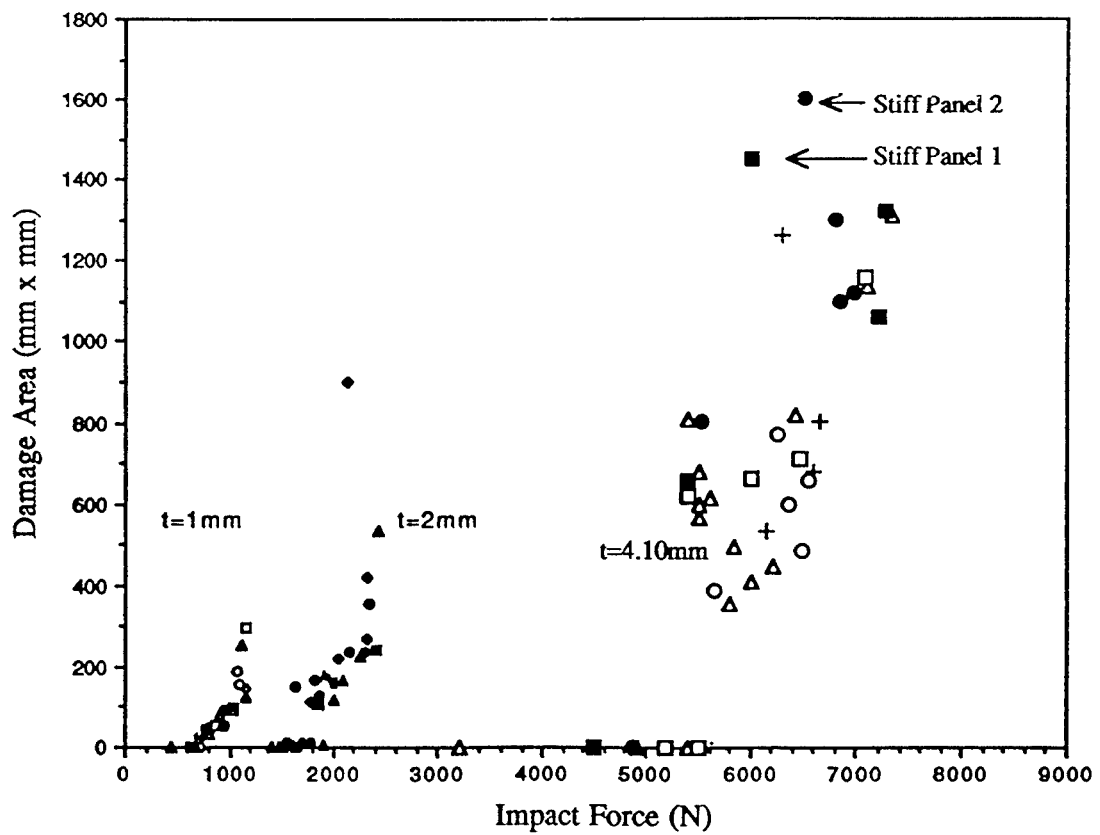
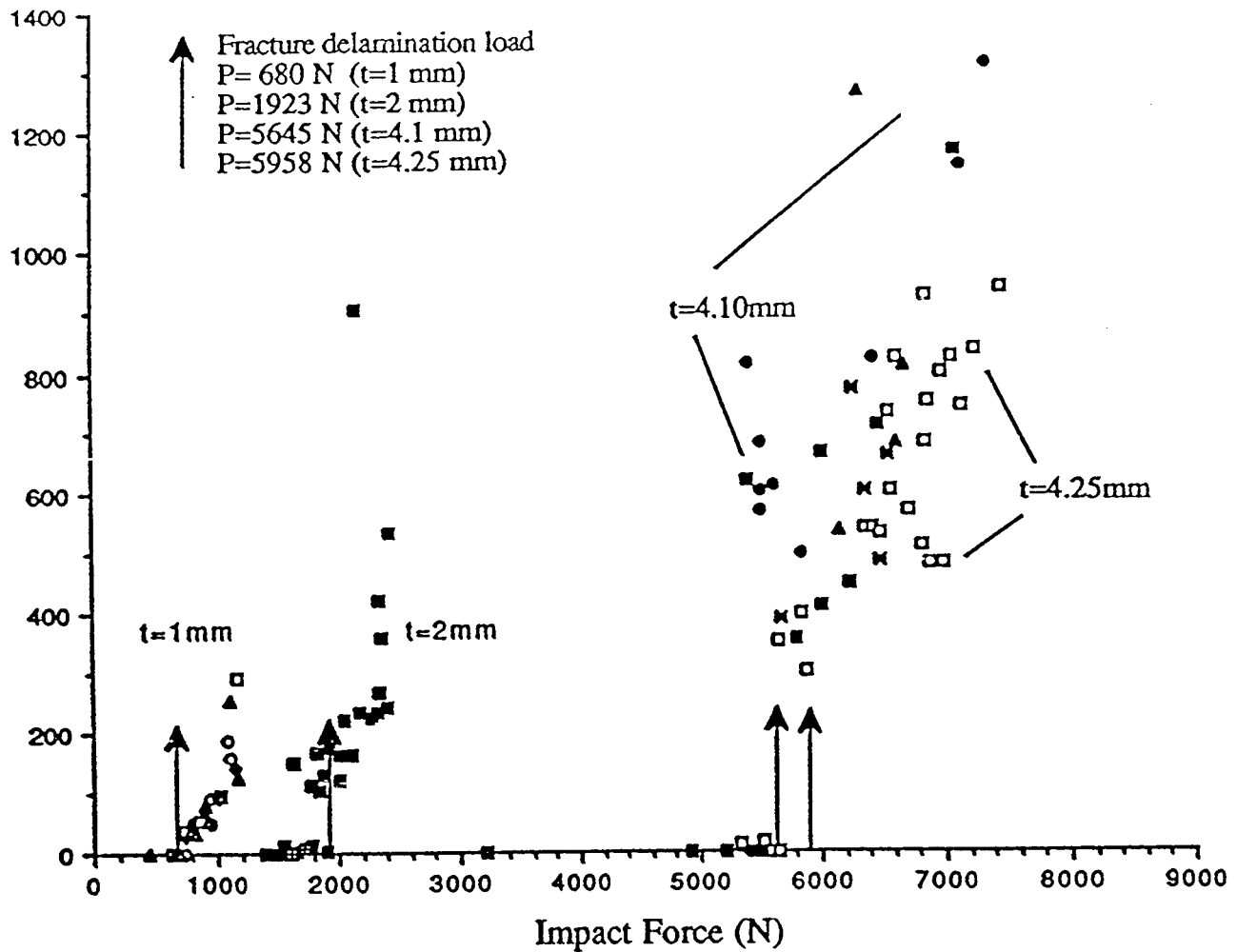


Figure 4(b) Map of damage against force

Fracture-based predictions for delamination in a variety of plate dimensions and support conditions



$$P_{crit}^2 = \frac{8\pi^2 Et^3 G_{IIC}}{9(1-\nu^2)}$$

Figure 5 Simple force threshold predictions

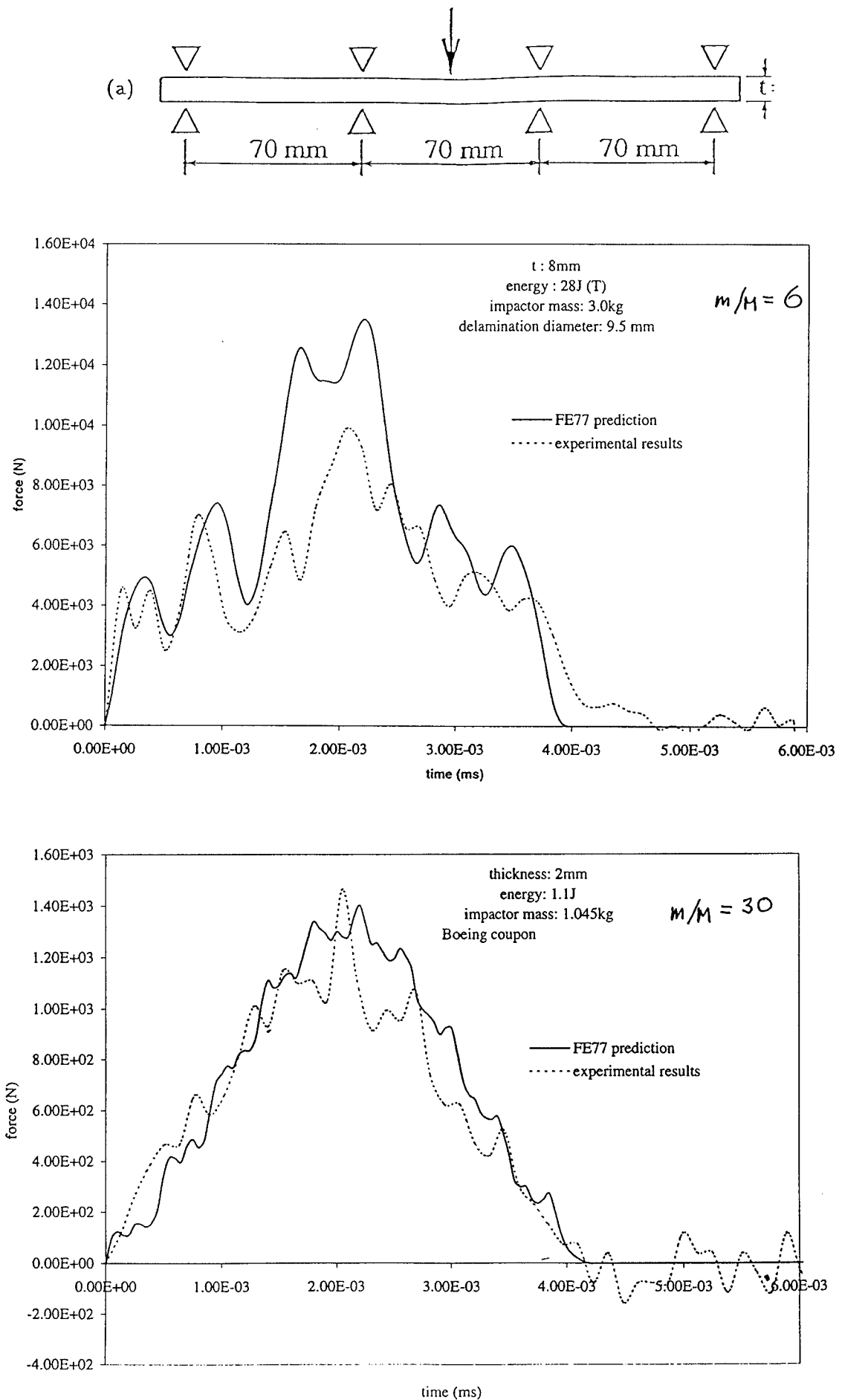
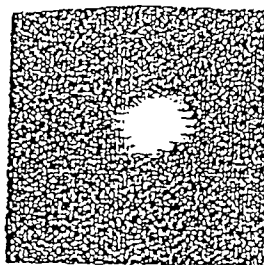
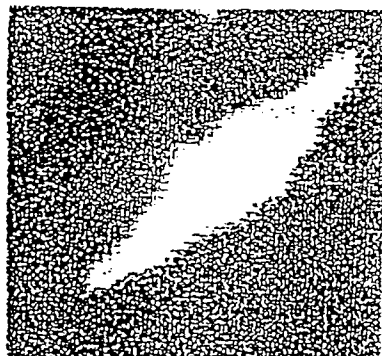
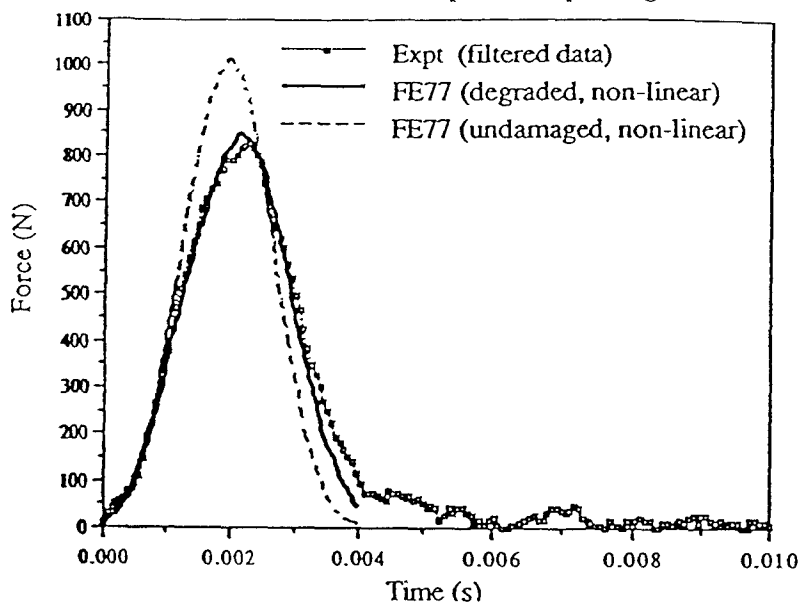


Figure 6 Effect of higher harmonic response
on force history



Test SC1-4a, small 1mm coupon, clamped edges, 0.88J



Test SC1-7a

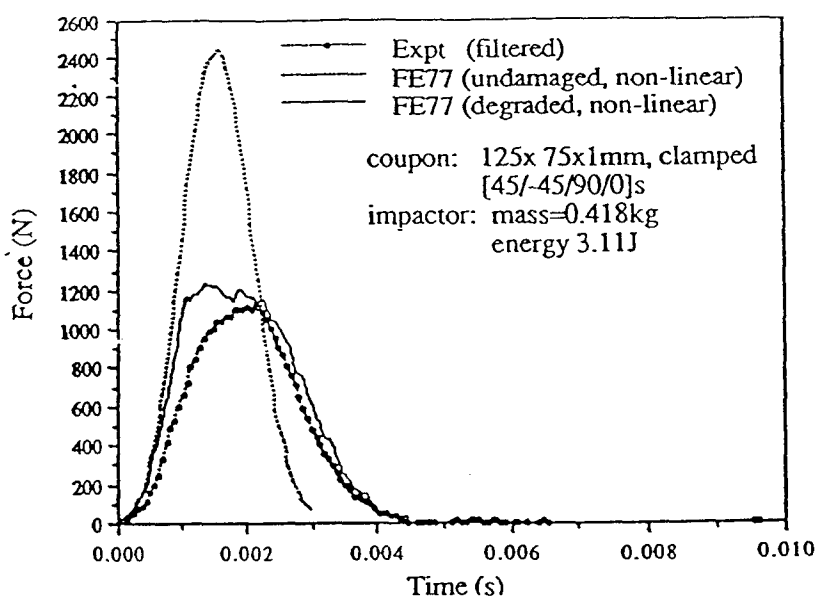
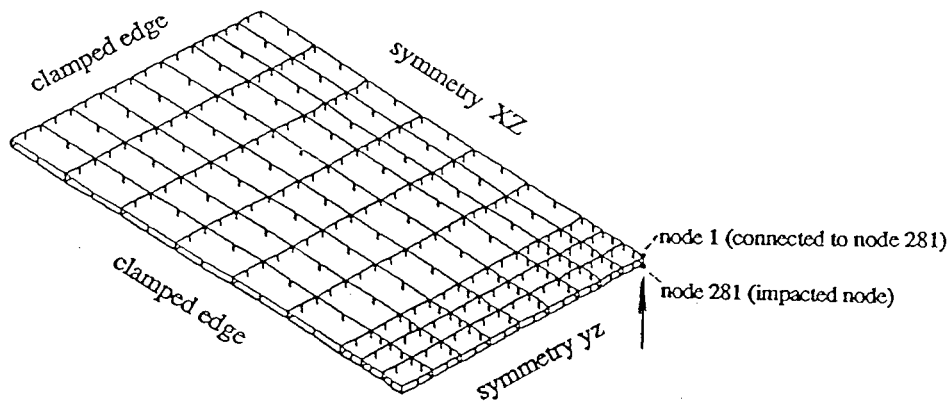


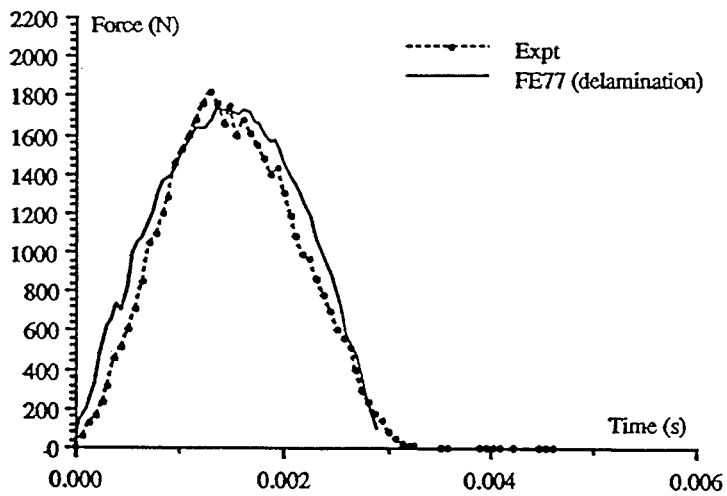
Figure 7 FE force predictions with and without extensive flexural damage

(a) 0.88J

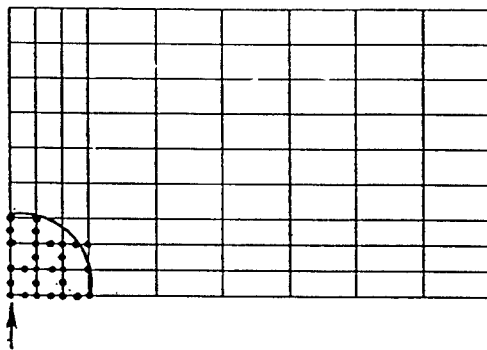
(b) 3.11J



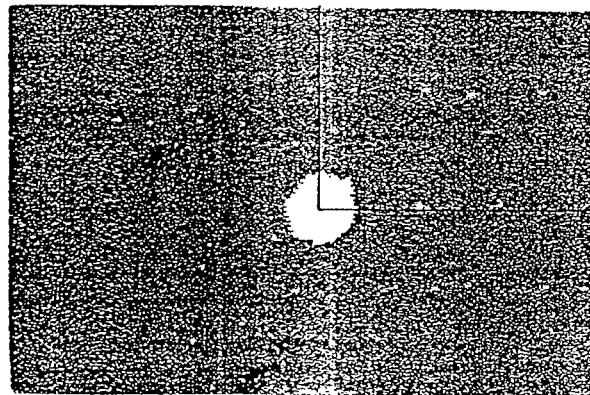
FE model of one quarter plate for delamination simulation.



Comparison of predicted and measured force histories.

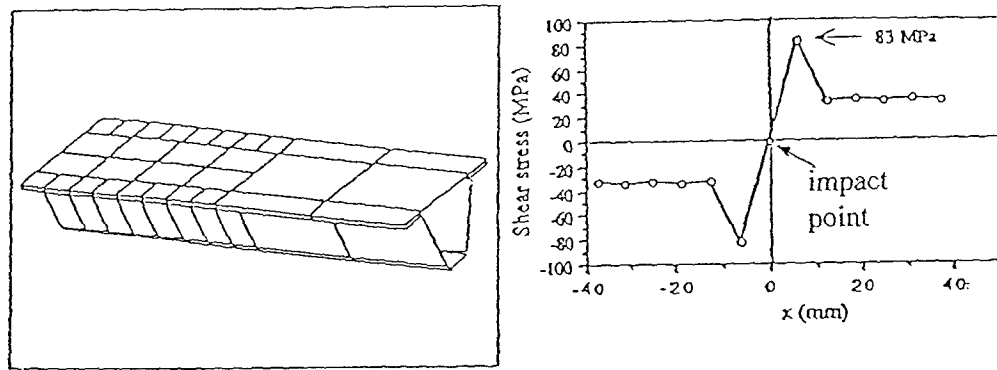


predicted delamination area = 160 mm².

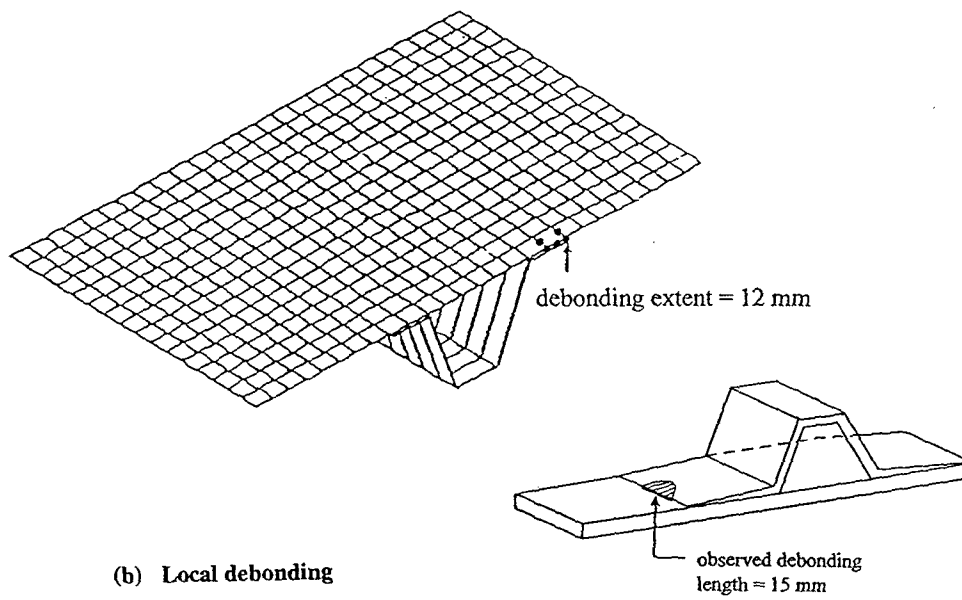


C-scan detected damage area = 140 mm².

Figure 8 Predictions of delamination size using just one array of breakable links



(a) Distribution of shear along the stiffener



(b) Local debonding

Figure 9 Prediction of debonding at stiffener interface

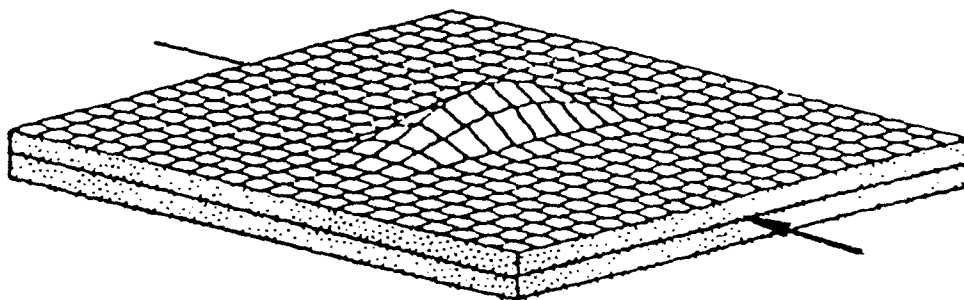


Figure 10 Buckling of delaminated zone

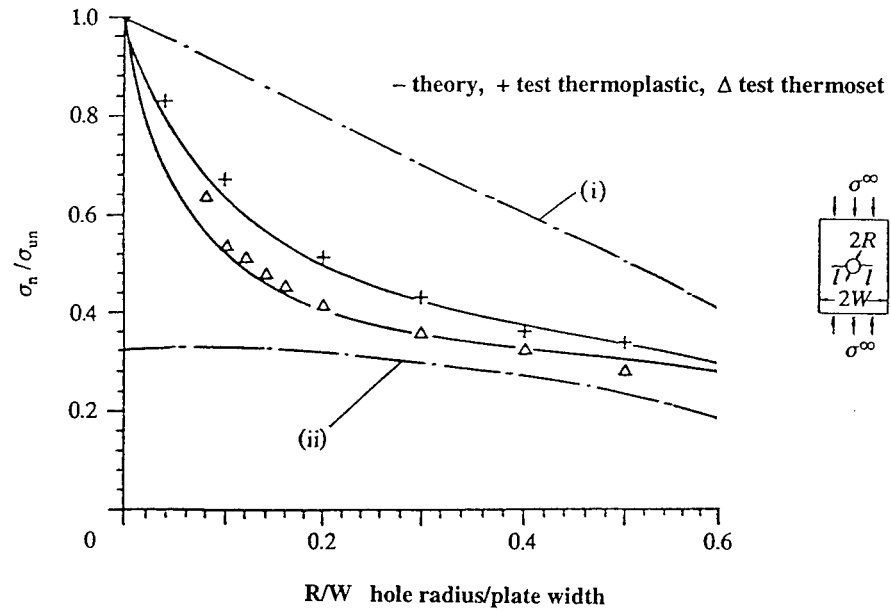


Figure 11 Open hole model for CAI prediction

(i) fully ductile material (ii) completely brittle material

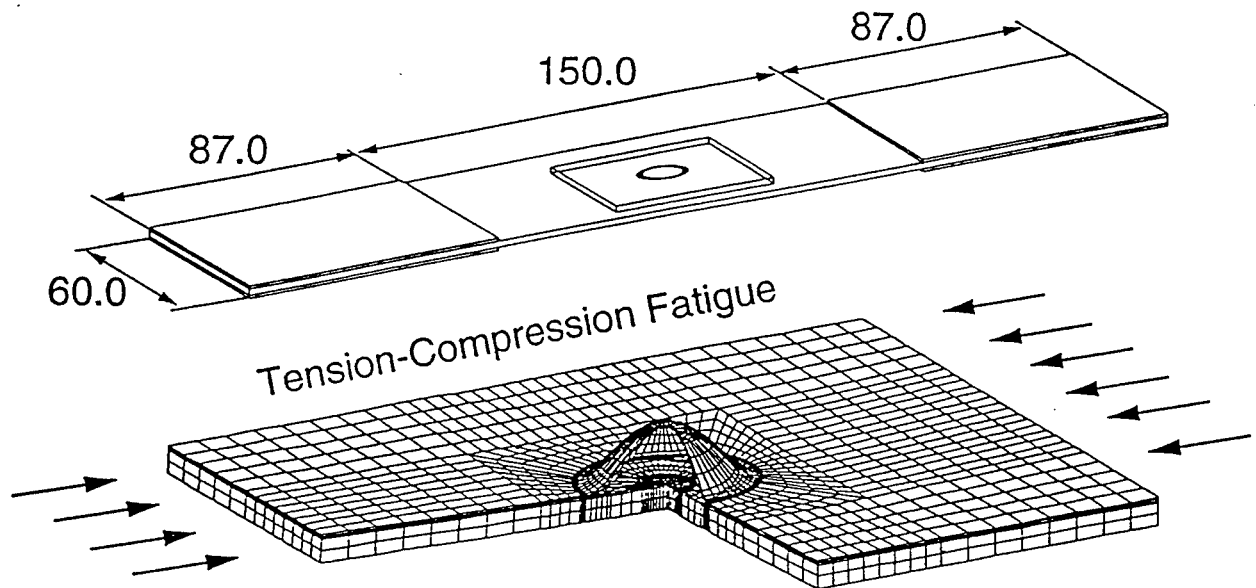


Figure 12 FE model for fatigue delamination [Ref. 9]